

Nano- and Micro-Auxetic Plasmonic Materials

João Valente,* Eric Plum,* Ian J. Youngs, and Nikolay I. Zheludev*

Auxetics, materials with a negative Poisson's ratio, are rare in nature. They possess the distinct mechanical property of expanding laterally upon being stretched which leads to important applications such as mechanical impact shields and particle filters. Several design concepts and fabrication techniques for artificial planar arrays of auxetic meta-molecules, with typical lattice parameters from millimeters to tens of micrometers, have been developed. Here we report, for the first time, planar auxetic materials with lattice parameters and optical properties of plasmonic metamaterials for the mid-infrared to optical part of the spectrum. These first auxetics with lattice parameters in the range from a few micrometers to hundreds of nanometers are fabricated by structuring a nanoscale plasmonic film supported by a dielectric nanomembrane. Under uniaxial tension or compression, our materials exhibit negative Poisson's ratios between -0.3 and -0.5 . Infrared and optical spectra of these structures show plasmonic resonances, indicating that such materials could act as novel nanomechanical light modulators.

In analogy to electromagnetic metamaterials, auxetics are often called mechanical metamaterials as their properties result from structuring. Negative Poisson's ratio,^[1–5] synclastic behavior,^[6] and wave-energy harvesting^[7] are examples of unique properties that mechanical metamaterials can exhibit. In contrast to normal materials, negative Poisson's ratio structures have the peculiar property that, when stretched in one direction, they will expand in the perpendicular direction. Numerous auxetic structures have been demonstrated theoretically^[3,4,8–10] and experimentally studied at millimeter to submillimeter^[11–16] and molecular scales.^[17] Suitable fabrication techniques are determined by the characteristic size of the auxetic structure. For example, macroscopic structures with unit-cell dimensions larger than 1 mm were fabricated using open cell polymeric or metallic foams,^[1] aramid paper,^[11] mechanical devices made of hinges, springs, and sliding collars,^[18]

and epoxy-resin casting.^[19] Soft lithography,^[12] femtosecond laser ablation,^[13] and digital micromirror device projection printing^[14] have allowed the fabrication of negative Poisson's ratio structures with characteristic sizes of hundreds of micrometers. Smaller dielectric auxetics with unit cells on the order of 100 μm have been made by laser micromachining,^[15] while dielectric auxetics with a characteristic size of 10 μm have been realized by direct laser writing.^[16] However, negative Poisson's ratio materials with nanoscale lattice parameters cannot be fabricated using such techniques due to their limited resolution and the complexity of auxetic designs. Nevertheless, nanoscale auxetics would be particularly interesting as optical materials, considering that the combination of transformation optics concepts^[20] with dielectric properties of auxetic metamaterials^[19,21–25] already promises better electromagnetic cloaking devices for microwaves.^[26,27]

Here, we realize micro- and nanoscale metamaterial structures and demonstrate negative Poisson's ratios by mechanical actuation (**Figure 1**). Our nano-auxetic metamaterials are based on the re-entrant honeycomb design, which is known for auxetic properties for a wide range of beam thicknesses, sizes, and angles.^[11] Inspired by recent work in the field of nanomechanical photonic devices,^[28] nanomembrane technology was used to fabricate auxetics with lattice parameters in the range from a few micrometers to hundreds of nanometers. Nanomembrane technology has already provided simple and efficient solutions for reconfiguration of nanoscale structures that are not auxetic, enabling nanomechanical devices and sensors. In particular, engineered resonant optical properties and anisotropic light modulation with up to 50% optical contrast has been demonstrated with reconfigurable metamaterials actuated by thermal,^[29] electric,^[30] and magnetic^[31] signals, and fabricated from plasmonic-thin-film-coated nanomembranes.

The auxetic materials are shown by **Figure 2** and were fabricated by thermally evaporating a 60 nm-thick gold plasmonic layer on a commercially available silicon nitride membrane of 50 nm thickness and then milling the re-entrant honeycomb structure through both layers using a gallium-focused ion-beam system (Helios 600 NanoLab by FEI). All structures were milled with an ion-beam energy of 30 keV. Infrared auxetic metamaterial microstructures were fabricated with 70 pA ion-beam current and a spot size of 21 nm, while nano-auxetic structures were milled with a reduced ion current of 9 pA and a smaller spot size of 12 nm. The honeycomb pattern has a rhombic unit cell and wallpaper symmetry group $cm\bar{m}$.^[32] For simplicity, we specify the smallest rectangular cell, $p_x \times p_y$, that describes each structure, where the periodicities p_x and p_y along x and y correspond to the diagonals of the elementary rhombic unit cell, see **Figure 3a**. The structure consists of horizontal beams of length $h \approx 0.8p_x$ forming an angle $\alpha \approx 60^\circ$ with beams of length $d \approx 0.4p_x$ as shown by **Figure 3a**. The auxetic microstructures for the infrared have $7 \mu\text{m} \times 5 \mu\text{m}$ rectangular cells, an overall size of $60 \mu\text{m} \times 60 \mu\text{m}$, and narrow ($w \approx 0.1p_x$) and wide ($w \approx 0.2p_x$) line widths of the honeycomb

J. Valente, Dr. E. Plum, Prof. N. I. Zheludev
Optoelectronics Research Centre
University of Southampton
Southampton SO17 1BJ, UK
E-mail: jpv1f11@orc.soton.ac.uk;
erp@orc.soton.ac.uk; niz@orc.soton.ac.uk

Prof. I. J. Youngs
Platform Systems Division
DSTL
Salisbury SP4 0JQ, UK

Prof. N. I. Zheludev
The Photonics Institute and Centre for Disruptive
Photonic Technologies
Nanyang Technological University
Singapore 637371, Singapore

This is an open access article under the terms of the Creative Commons Attribution License, which permits use, distribution and reproduction in any medium, provided the original work is properly cited.

The copyright line for this article was changed on 26 Aug 2016 after original online publication.

DOI: 10.1002/adma.201600088



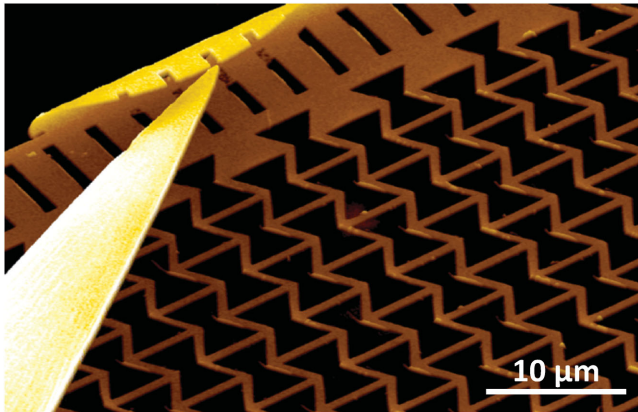


Figure 1. Metamaterial of the micro- and nano-auxetic family. SEM-based image of an auxetic structure actuated by a micromanipulator (on the left). The metamaterial is a mesh of nanowires cut from a nanoscale gold on silicon nitride membrane. The micromanipulator tip applies a force to the metamaterial by acting on the supporting beam (top left). Such micro- and nanoscale mechanical metamaterials exhibit strong plasmonic resonances in the infrared to optical parts of the spectrum as well as auxetic mechanical properties that are seen upon stretching and compression.

pattern, respectively, see Figure 2a,b. The nano-auxetics for the optical part of the spectrum are miniaturized versions of the latter with an overall size of $20\ \mu\text{m} \times 20\ \mu\text{m}$ and rectangular

cell dimensions of $1.8\ \mu\text{m} \times 1.2\ \mu\text{m}$ and $900\ \text{nm} \times 600\ \text{nm}$, see Figure 2c,d. Only two sides of the metamaterial structures are supported, by the gold-coated silicon nitride membrane on one side and an elastic beam on the opposite side to allow for actuation in the y -direction, as well as expansion and shrinking along the x -direction.

In order to measure the mechanical properties of the auxetic metamaterials, the larger and more robust arrays were actuated using a $100\ \text{nm}$ micromanipulator tip (Figure 1). The micromanipulator was used to move the elastic beam of $100\ \mu\text{m}$ length that supports one side of the structure resulting in a uniaxial force that stretches or compresses the entire metamaterial, depending on the direction of micromanipulator movement. We did not notice any significant buckling of the structures. The resulting axial and transverse strains were measured by scanning electron microscopy (SEM) observation of the structures in their deformed and relaxed states. All the experimental strains were smaller than 3% and our measurements show that the metamaterials expand laterally upon axial stretching and that they shrink laterally upon axial compression. Thus, the axial ϵ_{axial} and transverse ϵ_{trans} strains were found to have the same sign in all cases, corresponding to auxetic behavior and a negative Poisson's ratio $\nu = -\epsilon_{\text{trans}}/\epsilon_{\text{axial}}$. The deformation of the infrared auxetics with narrow (Figure 2a) and wide (Figure 2b) re-entrant honeycomb designs is best described by Poisson's ratios of $\nu_{\text{narrow}} = -0.51 \pm 0.06$ and $\nu_{\text{wide}} = -0.34 \pm 0.09$ for

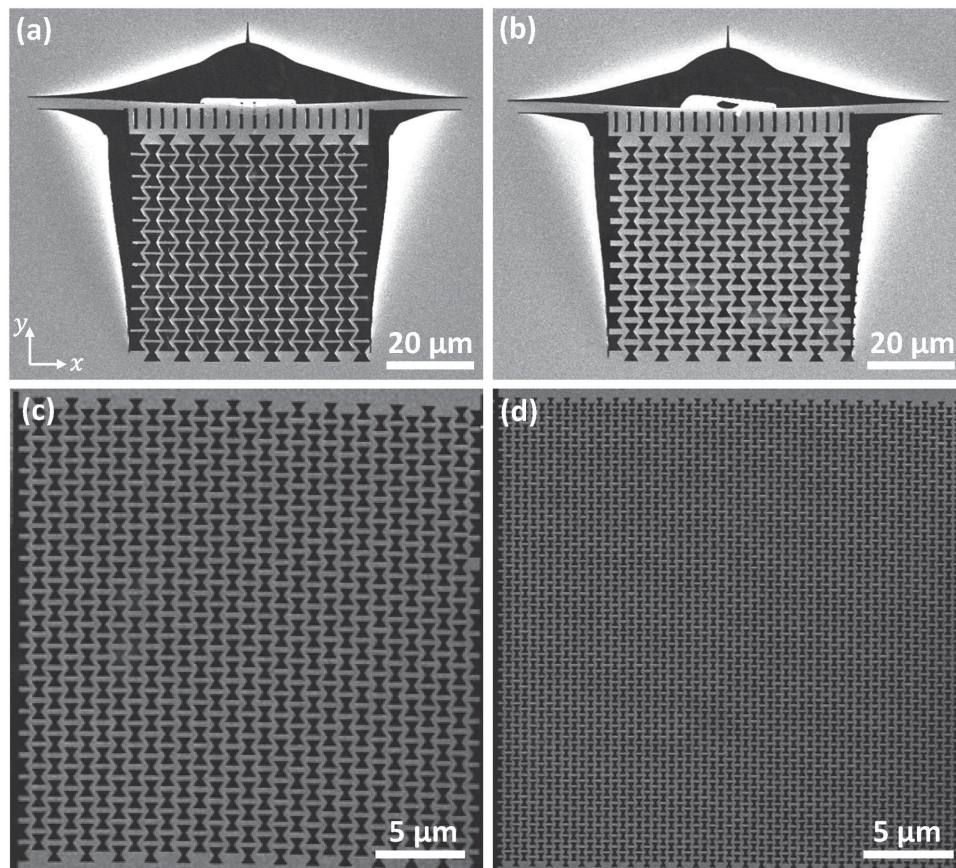


Figure 2. a–d) Scalable design of auxetic metamaterial with different dimensions of the rectangular cell: $7\ \mu\text{m} \times 5\ \mu\text{m}$ (a,b), $1.8\ \mu\text{m} \times 1.2\ \mu\text{m}$ (c), and $900\ \text{nm} \times 600\ \text{nm}$ (d). All structures are fabricated from a $110\ \text{nm}$ -thick gold-coated silicon nitride membrane.

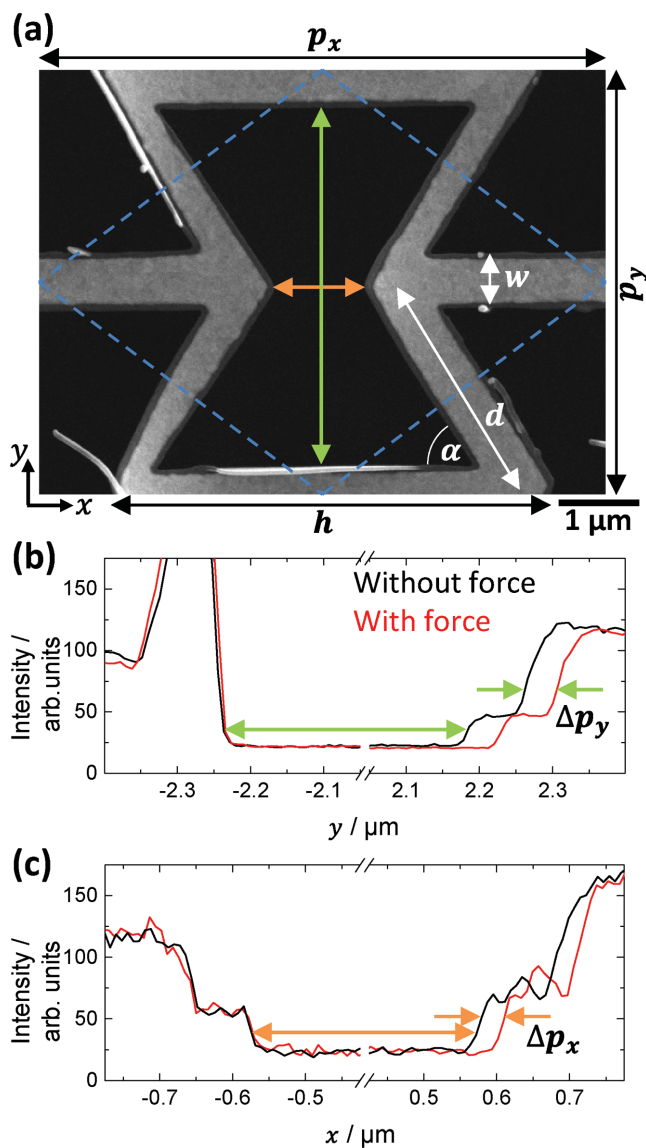


Figure 3. Strain measurements. a) Characteristic dimensions used in the analysis of strain under external force. One $7 \mu\text{m} \times 5 \mu\text{m}$ rectangular cell of the micro-auxetic of Figure 2a is shown. The structure's rhombic unit cell (blue dashed lines) and the honeycomb parameters p_x , p_y , h , d , w , and α are indicated. b,c) Example SEM image intensity cross sections along y and x as indicated by the green and orange arrows in panel (a). Cross sections recorded without (black) and with (red) application of external force along y indicate a force-induced increase of the unit cell size along both y and x .

both tension and compression within experimental accuracy. As the Poisson's ratio of structured materials does not depend on scaling the size of their unit cell,^[6,9] we argue that negative Poisson's ratios of approximately ν_{wide} shall also be expected in case of the more fragile nano-auxetics, which are miniaturized versions of the microscale re-entrant honeycomb design with wide beams. We note that 2D theoretical models assuming narrow beams ($w \ll d$) predict a Poisson's ratio close to -1 for our structures,^[3] however, the relatively wide beams of our auxetics ($w \approx d/4$ and $w \approx d/2$) are known to yield Poisson's ratios

of reduced magnitude.^[11] Out-of-plane deformation, that could occur as our beams are thin in the z -direction ($t = 110 \text{ nm} < w$), as well as fabrication imperfections may also contribute to deviations from the 2D models.

Measurements of nanoscale axial and transverse deformations of the metamaterial unit cells require precise measurements of length changes. Therefore, we determined length changes by analyzing SEM images recorded with and without micromanipulator actuation systematically. In order to avoid systematic errors, for a given metamaterial, images of a chosen unit cell were recorded in sequence with fixed magnification and various applied forces. The axial strain corresponds to the relative length change of the unit cell along the y -direction. As the re-entrant honeycomb unit cell has parallel gold edges (Figure 3a) that correspond to step-like transitions of the image intensity along y (Figure 3b), statistical errors of the gold edge separation along y were minimized by averaging the central part of the unit cell's image along x . Axial nanodisplacements due to force application can be seen clearly (Figure 3b) and the force-induced axial length change of the unit cell Δp_y has been extracted, where 1 pixel corresponds to 8 nm. The transverse strain corresponds to the relative length change of the unit cell along the x -direction Δp_x and therefore it is controlled by the force-induced gap change between the re-entrant parts of the unit cell (Figure 3c). In order to minimize statistical errors, this gap change was measured for multiple characteristic distances and then averaged.

Structuring of the metal–dielectric membrane controls not only its mechanical properties but also its optical properties. Due to the micro- and nanoscale nature of our structures, they are indeed effective media (electromagnetic metamaterials) when considering infrared and optical radiation with sufficiently large wavelengths to avoid diffraction. Metamaterials consisting of a simple rectangular lattice of unit cells diffract normally incident radiation if the wavelength is shorter than the longer of the rectangular unit cell dimensions p_x and p_y . Similarly, diffraction for rhombic lattices occurs when the wavelength of normally incident radiation is shorter than the separation $\lambda_c = p_x \sin(\tan^{-1} p_y / p_x)$ of the parallel sides of the rhombic unit cell (dashed lines in Figure 3a). Therefore, and due to the presence of a plasmonic thin film, typical metamaterial electromagnetic properties arise in such auxetic materials. The optical properties of metallic micro- and nanostructures, such as the auxetic metamaterials investigated here, are determined by the localized plasmonic response of coupled oscillations of conduction electrons and the electromagnetic near-field induced by the incident light. This is illustrated by Figure 4, which shows numerical simulations of the transmission and reflection spectra for the smallest auxetic nanostructure alongside the plasmonic excitations corresponding to selected spectral features (Comsol Multiphysics). The nano-auxetic exhibits a narrow absorption resonance (reflection minimum A) at about 870 nm wavelength, which corresponds to an anti-symmetric plasmonic excitation also known as “trapped” mode. These anti-symmetric plasmonic currents cannot radiate efficiently, as their radiated fields would cancel in the far-field and therefore electromagnetic energy is trapped by the auxetic metamaterial, resulting in large resonant plasmonic fields and about 50% absorption. At a wavelength of about 970 nm, the metamaterial becomes highly reflective

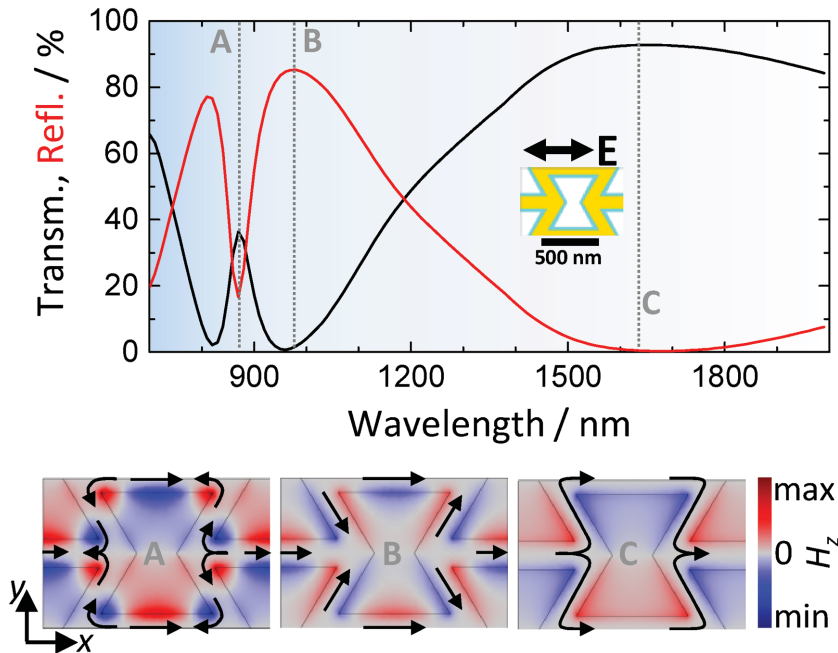


Figure 4. Plasmonic resonances of auxetic metamaterials. Simulated transmission (black) and reflection (red) spectra for the nano-auxetic metamaterial with rectangular cell size $900 \text{ nm} \times 600 \text{ nm}$. The direction of the electric polarization E of the incident wave is indicated. The color maps show the instantaneous magnetic field normal to the metamaterial plane H_z for selected spectral features A, B, and C. H_z is linked by Ampère's law to the optically induced instantaneous plasmonic currents, which are indicated by arrows.

(marked B), which is caused by a strongly scattering electric dipole mode, where the x -component of all plasmonic currents oscillates in phase. In contrast, reflectivity vanishes almost completely at around 1630 nm wavelength (marked C), due to a non-resonant anti-symmetric excitation of the nanostructure. The

same trapped mode absorption resonance (A), electric dipole reflection maximum (B), and non-resonant transmission window (C) are also seen in experimental transmission and reflection spectra of the auxetic metamaterials, see Figure 5. The latter were measured using Fourier transform IR ($3.0\text{--}11.0 \mu\text{m}$ wavelength) and vis-IR ($700\text{--}2000 \text{ nm}$) micro-spectrophotometers for the micro- and nanostructures, respectively. All auxetic metamaterials exhibit similar plasmonic transmission and reflection resonances in the non-diffracting regime. The strength and spectral position of these resonances depend on the size and structural details of the plasmonic honeycomb structure as well as the dispersion of the permittivity of gold. A reduction of the honeycomb line width shifts the resonant response further into the infrared (Figure 5a,b), while the spectral position of the resonances approximately scales with the overall size of the unit cell (Figure 5b–d). At this stage of research, we were not able to characterize the optical properties of the auxetic metamaterials under controlled actuation, which would require simultaneous measurements of optical properties and mechanical deformations. However, the plasmonic response and thus the optical properties of metamaterials have been shown to be highly sensitive to the geometry of the structure.^[28] We argue that also actuation of micro- and nanoscale auxetic metamaterials will lead to pronounced changes of their optical properties, such as changes of strength and spectral position of plasmonic resonances.

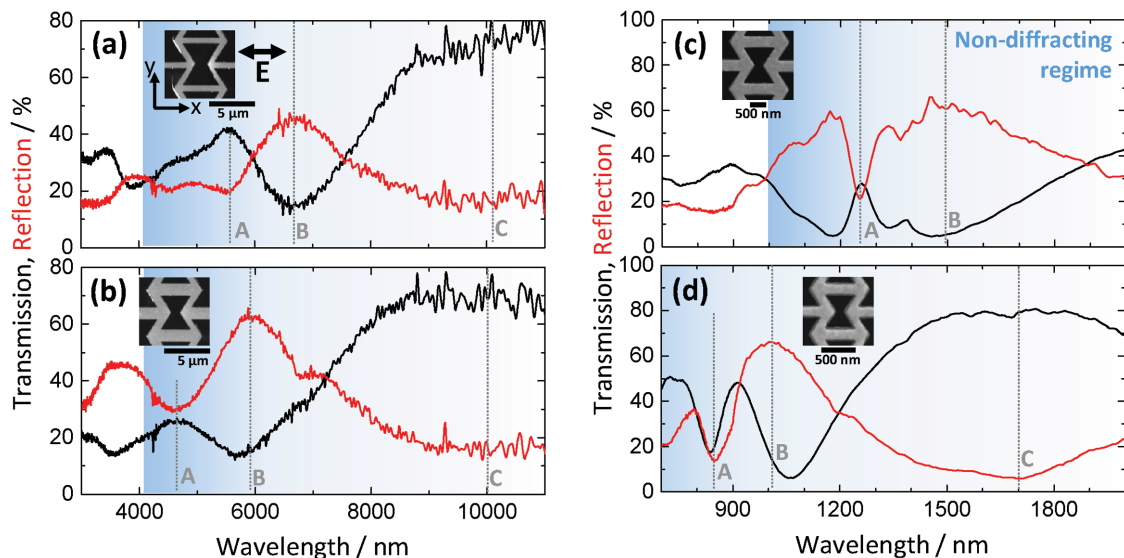


Figure 5. Optical properties of micro- and nano-auxetics. a) Measured transmission (black) and reflection (red) spectra for auxetic metamaterials based on the narrow line width re-entrant honeycomb pattern with a $7 \mu\text{m} \times 5 \mu\text{m}$ rectangular cell, and b–d) the corresponding wide line width pattern for rectangular cell sizes of: b) $7 \mu\text{m} \times 5 \mu\text{m}$, c) $1.8 \mu\text{m} \times 1.2 \mu\text{m}$, and d) $900 \text{ nm} \times 600 \text{ nm}$. Spectra are shown in the characteristic spectral ranges of the micro- and nanostructures, the direction of the electric polarization E of the incident wave is indicated, and plasmonic excitations corresponding to spectral features A, B, and C are shown by Figure 4.

Micro- and nano-auxetic metamaterials combined with actuation mechanisms of reconfigurable terahertz and photonic metamaterials^[30,31,33,34] promise a class of tunable nanomechanical metadevices with fixed optical anisotropy. In contrast to conventional materials and metamaterials, where stretching or compression necessarily changes the anisotropy of the structure, auxetics provide an opportunity where both the aspect ratio of the unit cell and its corresponding optical anisotropy (or isotropy) can in principle remain unchanged with actuation.^[18] Careful design of the auxetic scaffold that supports plasmonic or high-index dielectric resonators enables unique combinations of mechanical and optical properties that may be controlled through actuation with sub-microsecond response times.^[28] Recent advances in MEMS and NEMS reconfigurable metamaterials^[30,31,33] provide solutions for electrical actuation of micro- and nano-auxetic metamaterials, enabling applications in optoelectronic devices, e.g., tunable wave plates based on anisotropic auxetics, and polarization insensitive nanomechanical light modulators and variable filters based on isotropic auxetics. Miniaturization of such structures drives up achievable modulation speeds, which are expected to reach gigahertz on the nanoscale,^[28] and, in contrast to conventional reconfigurable metamaterials, auxetic devices could also benefit from enhanced mechanical properties such as fatigue and indentation resistance.^[35,36] We note that large optical modulation contrast may require large strains, which can lead to buckling in case of compression, however, such buckling will be reduced in structures consisting of narrower and thicker beams ($w \ll t$).

In summary, we merge mechanical and electromagnetic metamaterials at the nanoscale by fabricating plasmonic micro- and nano-auxetic metamaterials that exhibit both a negative Poisson's ratio and resonant optical properties controlled by the metamaterial structure. Micromanipulation confirms lateral expansion upon axial stretching of the re-entrant honeycomb design, and the microscale and nanoscale nanomembrane metamaterials have pronounced transmission and reflection resonances in the infrared and optical parts of the spectrum, respectively. Our findings indicate that reconfigurable auxetic metamaterials operating in the optical spectral range promise a broad range of unusual optomechanical properties which is yet to be explored.

Acknowledgements

This work was supported by the UK's Defence Science and Technology Laboratory (Grant No. DSTLX1000064081), the MOE Singapore (Grant No. MOE2011-T3-1-005), the Leverhulme Trust, and the UK's Engineering and Physical Sciences Research Council (Grant Nos. EP/G060363/1 and EP/M009122/1). The data from this paper can be obtained from the University of Southampton ePrints research repository: <http://dx.doi.org/10.5258/SOTON/385119>.

Received: January 7, 2016

Revised: March 17, 2016

Published online: May 3, 2016

[1] R. Lakes, *Science* **1987**, 235, 1038.

[2] K. E. Evans, *Endeavour* **1991**, 15, 170.

- [3] L. J. Gibson, M. F. Ashby, G. S. Schajer, C. I. Robertson, *Proc. R. Soc. London, Ser. A* **1982**, 382, 25.
- [4] I. G. Masters, K. E. Evans, *Compos. Struct.* **1996**, 35, 403.
- [5] G. N. Greaves, A. L. Greer, R. S. Lakes, T. Rouxel, *Nat. Mater.* **2011**, 10, 823.
- [6] Y. Liu, H. Hu, *Sci. Res. Essays* **2010**, 5, 1052.
- [7] M. Carrara, M. R. Cacan, J. Toussaint, M. J. Leamy, M. Ruzzene, A. Erturk, *Smart Mater. Struct.* **2013**, 22, 065004.
- [8] A. Kolpakov, *J. Appl. Math. Mech.* **1985**, 49, 739.
- [9] J. N. Grima, P.-S. Farrugia, R. Gatt, D. Attard, *Phys. Status Solidi B* **2008**, 245, 521.
- [10] J. C. Álvarez Elípe, A. Díaz Lantada, *Smart Mater. Struct.* **2012**, 21, 105004.
- [11] F. Scarpa, P. Panayiotou, G. Tomlinson, *J. Strain Anal. Eng.* **2000**, 35, 383.
- [12] B. Xu, F. Arias, S. Brittain, X. Zhao, B. Grzybowski, S. Torquato, G. Whitesides, *Adv. Mater.* **1999**, 11, 1186.
- [13] A. Alderson, J. Rasburn, S. Ameer-Beg, P. G. Mullarkey, W. Perrie, K. E. Evans, *Ind. Eng. Chem. Res.* **2000**, 39, 654.
- [14] D. Y. Fozdar, P. Soman, J. W. Lee, L.-H. Han, S. Chen, *Adv. Funct. Mater.* **2011**, 21, 2712.
- [15] U. D. Larsen, O. Sigmund, S. Bouwstra, in *Proc. Ninth Annual Int. Workshop on Micro Electro Mechanical Systems*, Vol. 6, IEEE, Piscataway, NJ, USA **1996**, p. 365.
- [16] T. Bückmann, N. Stenger, M. Kadic, J. Kaschke, A. Frölich, T. Kennerknecht, C. Eberl, M. Thiel, M. Wegener, *Adv. Mater.* **2012**, 24, 2710.
- [17] S. Pagliara, K. Franze, C. R. McClain, G. W. Wyld, C. L. Fisher, R. J. M. Franklin, A. J. Kabla, U. F. Keyser, K. J. Chalut, *Nat. Mater.* **2014**, 13, 638.
- [18] R. F. Almgren, *J. Elasticity* **1985**, 15, 427.
- [19] F. Smith, F. Scarpa, B. Chambers, *IEEE Microwave Guided Wave Lett.* **2000**, 10, 451.
- [20] U. Leonhardt, *Science* **2006**, 312, 1777.
- [21] F. Smith, *IEE Proc. Microwave Antennas Propag.* **1999**, 146, 55.
- [22] F. Scarpa, F. C. Smith, B. Chambers, G. Burriesci, *Aeronaut. J.* **2003**, 107, 175.
- [23] C. Lira, F. Scarpa, M. Olszewska, M. Celuch, *Phys. Status Solidi B* **2009**, 246, 2055.
- [24] P. Kopyt, R. Damian, M. Celuch, R. Ciobanu, *Compos. Sci. Technol.* **2010**, 70, 1080.
- [25] R. Ciobanu, R. Damian, I. Casian-Botez, *Comput. Stand. Interfaces* **2010**, 32, 101.
- [26] D. Shin, Y. Urzhumov, Y. Jung, G. Kang, S. Baek, M. Choi, H. Park, K. Kim, D. R. Smith, *Nat. Commun.* **2012**, 3, 1213.
- [27] D. Shin, Y. Urzhumov, D. Lim, K. Kim, D. R. Smith, *Sci. Rep.* **2014**, 4, 4084.
- [28] N. I. Zheludev, E. Plum, *Nat. Nanotechnol.* **2016**, 11, 16.
- [29] J. Y. Ou, E. Plum, L. Jiang, N. I. Zheludev, *Nano Lett.* **2011**, 11, 2142.
- [30] J. Y. Ou, E. Plum, J. Zhang, N. I. Zheludev, *Nat. Nanotechnol.* **2013**, 8, 252.
- [31] J. Valente, J. Y. Ou, E. Plum, I. J. Youngs, N. I. Zheludev, *Appl. Phys. Lett.* **2015**, 106, 111905.
- [32] D. Schattschneider, *Am. Math. Mon.* **1978**, 85, 439.
- [33] W. M. Zhu, A. Q. Liu, X. M. Zhang, D. P. Tsai, T. Bourouina, J. H. Teng, X. H. Zhang, H. C. Guo, H. Tanoto, T. Mei, G. Q. Lo, D. L. Kwong, *Adv. Mater.* **2011**, 23, 1792.
- [34] J. N. Grima, M. Caruana-Gauci, M. R. Dudek, K. W. Wojciechowski, R. Gatt, *Smart Mater. Struct.* **2013**, 22, 084016.
- [35] A. Alderson, K. L. Alderson, *Proc. Inst. Mech. Eng., Part G* **2007**, 221, 565.
- [36] Y. Prawoto, *Comput. Mater. Sci.* **2012**, 58, 140.